RSC Advances

RSC Advances

www.rsc.org/advances

ROYAL SOCIETY OF CHEMISTRY

www.rsc.org/advances

RSC Advances

ARTICLE

A non-covalent strategy for montmorillonite/xylose self-healing hydrogel

Xianming Qi,[a] Ying Guan,[a] Gegu Chen,[a] Bing Zhang,[a] Junli Ren,[b] Feng Peng[*a] and Runcang Sun[ab]

Self-healing capability of hydrogels has becoming a hot topic in the area of hydrogels research. An economical, convenient, ecofriendly, and reproducible approach of prepared self-healing xylose-based hydrogel was introduced in this article. First, methylguanidine hydrochloride was grafted onto the backbone of xylose by ethylene glycol as crosslinking agent, and then the xylose with guanidinium ion pendants on their peripheries was entangled with exfoliated layered anionic montmorillonite (MMT) clay nanoplatelets under the dispersion of sodium polyacrylate (PAAS), forming xylose-based hydrogels, which were connected by hydrogen bonds and intermolecular adsorption with internal spongy porous structure. The synthesized xylose-based hydrogels had rapid self-healing ability and showed good swelling property. The structure and morphology of the composite hydrogels were characterized by FT-IR and SEM. The compression stress-strain suggested that elasticity of xylose-based hydrogels increased with the increment of modified xylose solution, and the compression stress increased with the increasing concentration of modified xylose. Thermal gravimetric analysis (TGA) indicated that the composite hydrogels had good heat resisting property due to the added inorganic MMT. All those properties demonstrated that the composite hydrogels had the potential applications such as water absorbent, flame retardant, and other functional materials.

Introduction

With the decreasing of fossil-fuel, the attention of the world has been paid to investigate new biodegradable materials that are much less reliance on petroleum products than that on traditional materials.[1,2] Therefore, lignocellulosic biomass has become a new focus of research in recent years. It mainly consists of three parts: lignin, cellulose, and hemicelluloses, which are all inexhaustible source of energy, with the nature of renewable, non-toxic and biodegradation. Xylose is a pentitol obtained from the xylan-rich portion of hemicelluloses from plants.[3] It is the most important raw materials for manufacturing xylitol. Xylose can be used as a food additive on account of its health function,[4] and it is also used as a no-calorie sweetener, because it can't be absorbed by the body.[5] In addition, xylose can be used as a platform chemical for the production of industrially important chemicals.[6]

A prosperous research field has formed in biomass-based hydrogels as a result of their widely potential applications, such as super absorptive materials, immobilization of enzyme, vehicles for drug delivery in pharmaceutical and medical science.[7,8] Furthermore, because of their good biocompatibility and ability to realize some of the functions of human tissues, some hydrogels have been applied to biomedical application.[9,10]

Given the environmental deterioration, it's reasonable to replace some petroleum-based plastics with biomass-based gels. Hydrogels are three-dimensional networks of crosslinked molecules that the vast majority of their mass consists of water, yet they still exhibit solid-like mechanical properties.[11] Hydrogels can be classified into two categories depending on whether the crosslinked gel networks use covalent or non-covalent approach.[12] Covalent hydrogels are rather fragile, having poor transparency and unable to autonomous heal once the network structure is broken because of the polymer chains interconnected by permanent non-reversible bonds.[13] To overcome these limitations, hydrogels formed through non-covalent and physical associations arising from hydrogen bonds and intermolecular interactions, instead of covalent crosslinks, have attracted significant interest recently. A new class of "aqua materials" has demonstrated that significant improvement in the mechanical properties of hydrogel is possible.[12] Aqua materials have large mechanical properties with high content of water and ultralow content of components; in addition, they can be molded into self-standing objects. More recently, hybridization of polymers with clay nanosheets (CNSs), so-called nanocomposite hydrogels, are capable of displaying good mechanical properties and optical transparency.[14] Montmorillonite (MMT), natural minerals, is composed of stacked layers of aluminum octahedron and

silicon tetrahedrons.[15] These layered silicates contain dangling hydroxyl end groups that can form hydrogen bonds with water, which make MMT highly hydrophilic.[16] Furthermore, MMT can be used as a reinforcing agent because of its good capability of exfoliation and dispersion in polymer matrices.[17,18]

Herein, we report a strategy for the formation of non-covalent hydrogel, on account of its outstanding features for convenient, quick, and reproducible preparation and the capability of self-healing. Guanidinium ions were grafted onto the backbone of xylose to obtain the modified xylose. Sodium polyacrylate (PAAS) was used as the dispersant for MMT suspension. The xylose-based hydrogels were prepared by mixing the modified xylose with MMT/PAAS suspension, and the properties of the composite hydrogels were further investigated in this study.

Materials and methods

Materials

Xylose was purchased from Beijing Aoboxing Bio-tech Co., Ltd. Methylguanidine hydrochloride was obtained from Tokyo chemical industry Co., Ltd. MMT, a naturally occurring mineral salt with a layered structure, was obtained from Alfa Aesar. PAAS (Molecular weight$\geq 3 \times 10^7$) was purchased from Sinopharm Chemical Reagent Co. Ltd. Ethylene glycol, analytical grade, was purchased from Beijing Chemical Works. All reagents mentioned above were directly used without further purification.

Preparation of modified Xylose

First, xylose (4.0 g) was dissolved in 20 mL of distilled water with vigorous mechanical stirring at 60 °C for 20 min. When the xylose was dissolved, ammonia water was added into the solution to adjust pH to 11; then the crosslinking agent, 0.5 mL of ethylene glycol was added into the solution, keeping heating at 60 °C for 25 min. After that, 1.5 g of methylguanidine hydrochloride was added to the solution and the mixture continued to be heated under stirring at 60 °C for 2.5 h. A desired amount of ethylene glycol (0.5 mL) was added again and stirred for another 2 h. Finally, the reaction mixture was settled down volatilization for one week at room temperature to obtain the modified xylose crystals. Fig. 1 shows the synthetic mechanism of the modified xylose.
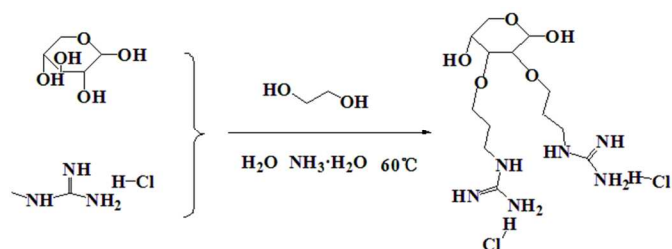
Fig. 1 Synthetic mechanism of modified xylose for grafting methylguanidine hydrochloride.

Preparation of MMT suspension

MMT (2.0 g) was first dispersed in distilled water (38 mL) with vigorous mechanical stirring at room temperature for 30 min, followed by ultrasonication for 15 min, and then continue to be stirred for 30min. This process was repeated four times. After storage of the MMT solution overnight, the undissolved solids were removed by centrifugation to obtain a homogeneous suspension of MMT (w%, 3.98%), which was used for the preparation of composite hydrogels.

Preparation of xylose-based self-healing hydrogels

As a typical hydrogel preparation, 5 mg/mL of PAAS solution was prepared by dissolving a certain amount of PAAS in aqueous solution. 1.0 mL of PAAS solution was added into the stirred suspension of MMT (3.0 mL) at room temperature. After about 10 min, the mixed suspension turned to a viscous solution owing to exfoliation of MMT. Then 0.1 mL of aqueous solution of modified xylose (50 mg/mL) was added dropwise by using an injector while stirring. The mixed solution became stiff immediately, forming a self-standing object, labeled as G-0.1. Other hydrogels were prepared similarly as mentioned above, using different volume of modified xylose solution such as 0, 0.3, 0.5, and 0.7 mL, coded as G-0, G-0.3, G-0.5, and G-0.7, respectively (Table 1). In addition, the hydrogels with different concentration of modified xylose solution were also prepared such as 30, 50, 70, and 90 mg/mL, labeled as H-30, H-50, H-70, and H-90, respectively (Table 2). To explore the properties of hydrogel without MMT, 0.4mL of modified xylose solution (90mg/mL) was directly added into the stirred 3ml of PAAS solution without MMT; however, the composite hydrogel was not formed due to the absent of MMT.

Table 1 Hydrogels with different volume of modified xylose.

Sample code	MMT	PAAS	Modified xylose
	V (mL)	V (mL)	V (mL)
G-0	3	1	0
G-0.1	3	1	0.1
G-0.3	3	1	0.3
G-0.5	3	1	0.5
G-0.7	3	1	0.7

The concentration of MMT, PAAS, and modified xylose solution was 3.98%, 5 mg/mL, and 50 mg/mL, respectively.

Table 2 Hydrogels with different concentration of modified xylose.

Sample code	MMT	PAAS	Modified xylose
	C (w%)	C (mg/mL)	C (mg/mL)
H-30	3.98	5	30
H-50	3.98	5	50
H-70	3.98	5	70
H-90	3.98	5	90

The volume of MMT, PAAS, and modified xylose solution was 3, 1, and 0.4 mL, respectively.

FT-IR spectroscopy

FT-IR spectra of the samples were carried out on Thermo Scientific Nicolet iN 10 FT-IR microscope with FT-IR spectrometer from 4000 to 650 cm^{-1} at a resolution of 4 cm^{-1} and 128 scans per sample.

Swelling capacity measurements

The freeze-dried composite hydrogels were weighed and then were immersed into distilled water to test swelling capacity at room temperature. The swollen hydrogels were took out and filtered with nylon fabric bag filter for 20 min until no free water dripped, then weighed at regular intervals until the composite hydrogels reached swelling equilibrium. The equilibrium water absorption was calculated as followed equation:

$$Q_{eq}=(W_2-W_1)/W_1$$

Where Q_{eq} is the equilibrium water absorption defined as grams of water per gram of sample. W_1 and W_2 are the mass of hydrogel samples before and after swelling, respectively.

SEM analysis

The section structures of the composite hydrogel were measured by scanning electron microscope (SEM, HitachiS-3400NII) to observe the internal microstructure. Images were obtained dependent on the feature to be traced.

Mechanical test

The composite hydrogels were shaped to cylindrical samples, and compression stress-strain tests were recorded using compressive tester (CTM6503, Shenzhen SANS Technology stock Co., Ltd. China) at a compression speed of 5 mm/min.

Thermal analysis

The thermal property analysis curves of xylose-based self-healing hydrogels were carried out by thermal gravimetric analysis (TGA) with temperature ranging from 20 to 600 °C at a ramp rate of 20 °C/min.

Results and discussion

The reaction mechanism

The reaction mechanism of hydrogelation is illustrated in Fig. 2. Firstly, the guanidinium ion pendants were introduced to the backbone of the xylose chain by cross-linking reaction, which could be used for the preparation of hydrogels with MMT, because the surfaces were full of anions[12]. MMT is a kind of natural minerals with 2:1 layered silicate crystal structure, and the interlayer cations are easily exchanged with inorganic or organic cations (Fig. 2a).[19] When MMT are mixed with PAAS

in water, they were highly entangled together and dispersed because of the mutual repulsion resulted from a possible site-specific wrapping of their positive-charged edge parts with anionic PAAS (Fig. 2b).[20] The modified xylose is dendritic molecular that contains multiple guanidinium ion pendants on their peripheries. Therefore, the modified xylose dispersed with MMT/PAAS suspension can strongly interact by non-covalent interaction between the guanidinium ion pendants and oxyanion surface groups, including hydrogen bonds and electrostatic interactions.[21-23] Then the good mechanical and self-healing hydrogel is formed quickly with well-developed network (Fig. 2c).
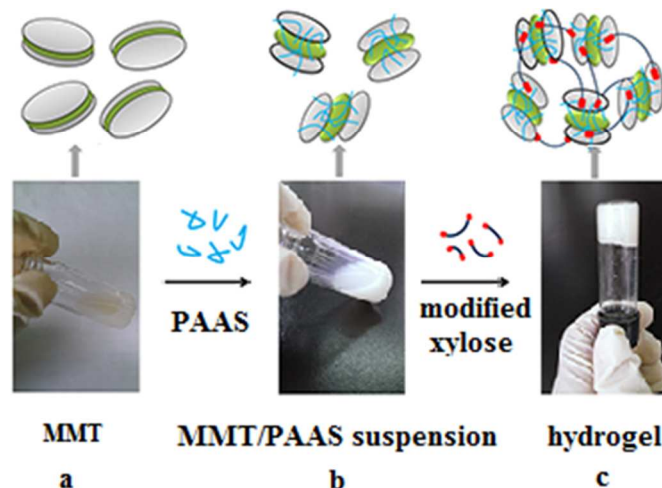
Fig. 2 Schematic representation of the mechanism of hydrogelation.

FT-IR analysis
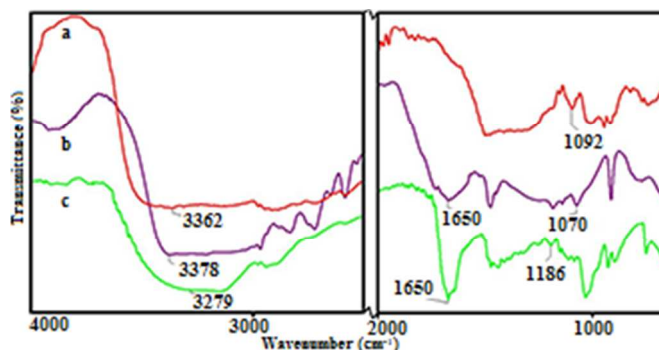
Fig. 3 FTIR spectra of xylose (a), methylguanidine hydrochloride (b) and modified xylose (c).

FT-IR spectroscopy was carried out to monitor the crosslinking process and the resulting products. Fig. 3 shows the FT-IR spectra of xylose (spectrum a), methylguanidine hydrochloride (spectrum b), and the modified xylose (spectrum c). In Fig. 3a, the absorption peak at 3362 cm^{-1} is corresponding to the -OH stretching vibration. The band at 1092 cm^{-1} is originated from the C-O-C stretching vibration.[24] In the FT-IR spectrum of methylguanidine hydrochloride (spectrum b), the bands at 3378, 1650, and 1070 cm^{-1} are assigned to -NH, -NH$_2$, and C-NH$_2$ vibration, respectively. In the FT-IR spectrum of the modified xylose, graft of xylose with

methylguanidine hydrochloride, is shown in Fig. 3c. The observed broad absorption band at 3279 cm^{-1} is due to the overlap of the -OH stretching of xylose and the -NH stretching of methylguanidine hydrochloride.[25] The signals at 1650 cm^{-1} is assigned to the vibration of -NH$_2$, which is consistent with the absorption peaks of methylguanidine hydrochloride. Besides, the new appeared absorption peak at 1186 cm^{-1} is attributed to the stretching vibration of the new bond C-C-N between xylose and methylguanidine hydrochloride. Therefore, the results of the spectra indicated that the xylose was modified successfully.

The FT-IR spectra of modified xylose, PAAS, MMT, hydrogels G-0, and G-0.5 are shown in Fig. 4. In the spectrum of PAAS (Fig. 4b), the frequency of the vibrational band at 2919 cm^{-1} is assigned to the -CH$_2$ stretching. The two different stretching vibrations at 1590 and 1440 cm^{-1} are corresponding to the carboxylate (COO$^-$). In the spectrum of MMT (Fig. 4c), the peak at 3620 cm^{-1} is attributed to the group of Al-OH stretching vibration.[26] A strong peak at 1634 cm^{-1} is assigned to the -OH bending vibration. The characteristic peaks at 991 and 834 cm^{-1} are indicative of the stretching vibration of Si-O-Si and Si-O-Al, respectively.[27]
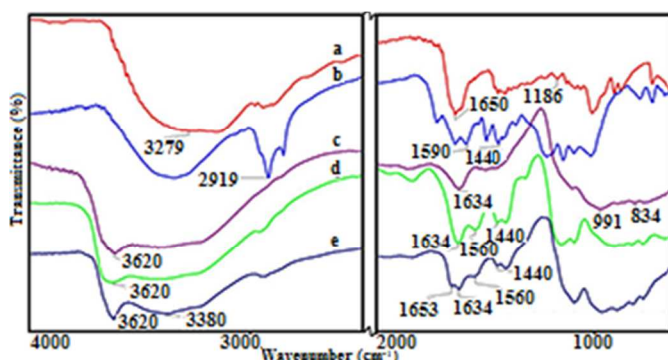
Fig. 4 FTIR spectra of modified xylose (a), PAAS (b) and MMT(c), hydrogels G-0 (d), and G-0.5(e).

The FT-IR spectra of hydrogels G-0 and G-0.5 are shown in spectrum d and spectrum e in Fig. 4, respectively. The absorption peaks at 3620, 1634 cm^{-1} both in hydrogels G-0 and G-0.5 are consist with the absorption peaks of MMT, and the signals at 1560, 1440 cm^{-1} both existed in hydrogels G-0 and G-0.5 are originated from the carboxylate (COO$^-$) vibration of PAAS. The featured bands suggested that the hydrogel G-0 was just formed by physically crosslinking by PAAS entangled with MMT. Furthermore, in the spectrum of hydrogel G-0.5, a new broad absorption band at 3380 cm^{-1} is assigned to the overlap of the -OH stretching vibration of xylose and the -NH stretching vibration of methylguanidine hydrochloride. The vibration at 1653 cm^{-1} is due to -NH$_2$ of methylguanidine hydrochloride. Based on the analysis above, the results indicated that carboxyl and guanidinium ions were introduced to the backbone of hydrogel G-0.5, which are benefit to form abundant of hydrogen bonds.[28,29] The internal hydrogel G-0.5 are crosslinked by noncovalent interactions, which endow the xylose-based hydrogel with rapid self-healing functionality.[30]

Self-healing process of xylose-based hydrogel

The process of self-healing of xylose-based hydrogel is illustrated in Fig. 5. As is shown in Fig. 5a, it was found that the composite hydrogel had good plasticity and could be molded into a certain shape. The prepared intact hydrogel was cut into two parts as shown in Fig. 5b. Then the ruptured surfaces were pressed together (Fig. 5c), and the fractured pieces merged autonomously into a single piece within a few minutes, which was attributed to plenty of reversible non-covalent bonds of hydrogen bonds and electrostatic adsorption. When the interface of the two recombined sections was dangling placed, the self-healing composite hydrogel could withstand its self-weight and the self-healing junction surface of the hydrogel could be found clearly in Fig. 5d. These illustrations revealed that the xylose-based hydrogels exhibited the self-healing ability and mechanical properties reversibility.
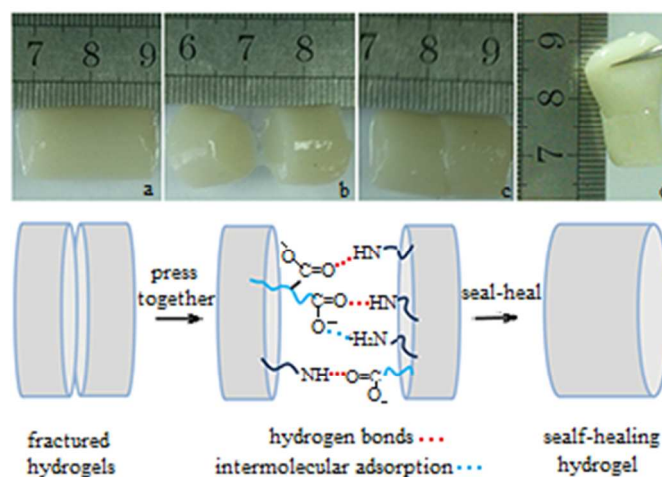
Fig. 5 Self-healing process of xylose-based hydrogel.

Swelling behaviors of xylose-based hydrogels
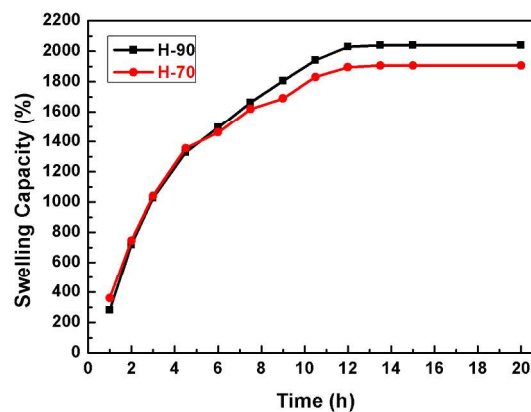
Fig. 6 Swelling capacity of hydrogels H-70 and H-90.

Swelling capacity is a reflection of hydrogel crosslinking density and internal structure,[31,32] the swelling behavior was detected for further investigating the structural features of the xylose-based hydrogels. The swelling capacity of xylose-based hydrogels H-70 and H-90 were shown in Fig. 6, respectively. It

was found that the swelling ratio gradually increased from 0 to 14 h and reached equilibrium after immersion for 16 h, which indicated that the composite hydrogels achieved the swelling equilibrium in a relatively short period of time. Besides, hydrogels H-70 and H-90 demonstrated the similar swelling curves within the first few hours, but the hydrogel H-90 showed a better swelling equilibrium with the swelling time increasing on account of more guanidinium ions were added, forming more hydrophilic groups with MMT/ PAAS suspension.

Morphological analysis

The interior crosslinked structure of the xylose-based hydrogel can be characterized by scanning electron microscopy (SEM). Fig. 7 shows the SEM images of the hydrogel H-90. Image a, b, c and d are obtained at magnifications of 200×, 500×, 800×, 1200×, respectively. As is shown from the image a, it was clearly found that the interior

of the hydrogel H-90 are composed of plentiful honeycomb structures. It resulted in that the composite hydrogel is soft and flexible. Besides, in image b and c, the morphology of hydrogel H-90 consisted of abundant micropores and lamellar structures with the tight network, and these porous structures were presumably the hydrophilic groups. The MMT particles were not found on the surface of the gel structures, which suggested that the MMT nanosheets were completely dispersed into the hydrogels without aggregation because of the interactions between the anion groups of MMT and guanidinium ion pendants of the modified xylose.[33] Moreover, the tight network among the molecular chains of the crosslinked polymer was caused by the crosslinking reaction, which resulted in that the pores became small and interconnected network dense. These porous and spongy dense structures were probably responsible for swelling and rapid self-healing of the xylose-based hydrogels.
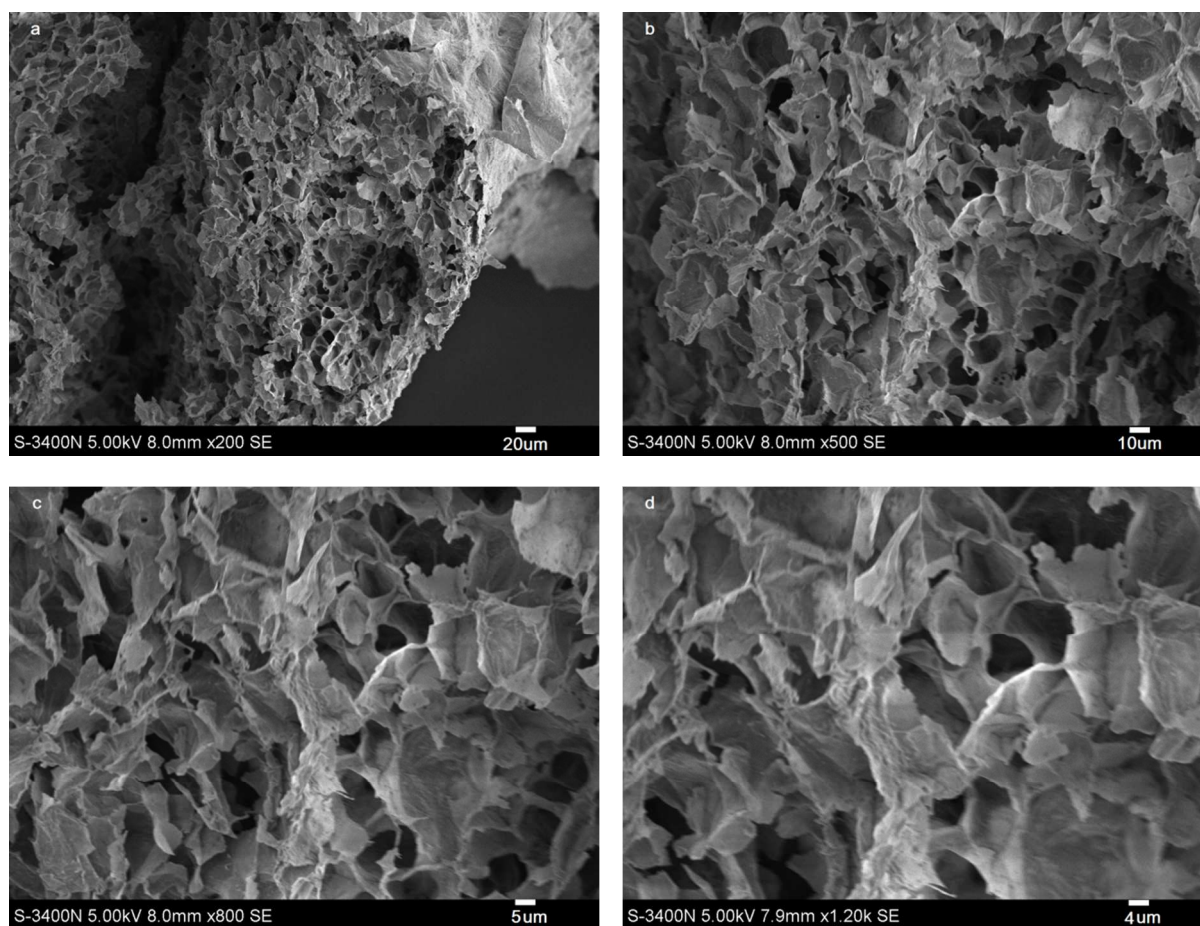
Fig. 7 SEM images of hydrogel H-90.

Mechanical properties of xylose-based hydrogel

The cylindrical composite hydrogel samples were tested to record the compression stress-strain curves. The compression stress-strain curves on behalf of the mechanical properties of hydrogels G-0, G-0.1, G-0.3, G-0.5, and G-0.7 are shown in Fig. 8. The compression stress of all the composite hydrogels increased slightly with the increasing deformation and all the

five samples showed the remarkably similar curves despite of the different volume of modified xylose solution. It indicated that these composite hydrogels had good elasticity and ductile property because of the hydrogen bonds and the electrostatic interactions. When the strain exceeded 50%, the whole compression stress-curves increased sharply. In addition, compared with the different compression stress-curves, the strain increased with the increasing volume of modified xylose

at the same compression stress. At the compression stress of 100 kPa, the strain of the hydrogel G-0 was 58.7%, and the other strain of the composite hydrogels were 64.2% (G-0.1), 65.1% (G-0.3), 67.1% (G-0.5), and 87.6% (G-0.7), respectively, which indicated that the plasticity of the prepared hydrogels increased with the added volume of modified xylose.
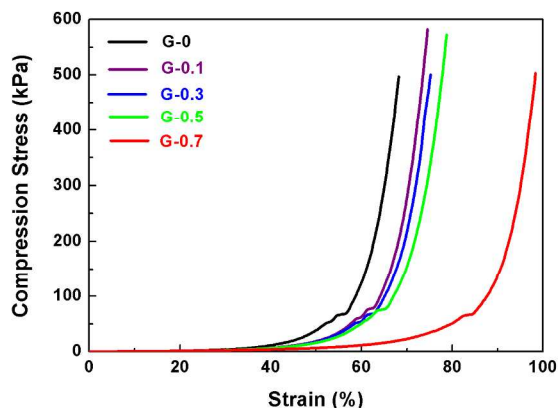
Fig. 8 Compression stress-strain curves of hydrogels G-0, G-0.1, G-0.3, G-0.5, and G-0.7.

The compression stress-strain curves of hydrogels H-30, H-50, H-70, and H-90 are shown in Fig. 9. As can be seen from Fig. 9, the strain increased with the decreasing concentration of modified xylose from H-90 to H-30 at the same compression strength. However, the compression stress increased from H-30 to H-90 at the same strain. At the strain of 75%, the compression strength of the hydrogels were 130 (H-30), 154 (H-50), 272 (H-70), and 336 kPa (H-90), respectively. The reason was that the higher concentration of the modified solution was added, more hydrogen bonds and the electrostatic interactions were formed during the preparation of the hydrogels, which suggested that the interior network structure of the xylose-based hydrogels was well crosslinked.

Compared Fig. 8 with Fig. 9, it was found that the strain of the composite hydrogels increased with the increment volume of modified xylose solution from G-0 to G-0.7 in Fig. 8. However, the strain of the composite hydrogels decreased with the increasing concentration of modified xylose from H-30 to H-90 in Fig. 9. The obvious differences in stress-strain of the hydrogels were possibly caused by the different water content in the composite hydrogels. Because the high water content in hydrogels can promote the elasticity of the composite hydrogels. Modified xylose was firstly dissolved in distilled water and then stirred with MMT/PAAS suspension to form hydrogels. The water content of the composite hydrogels increased with the increment of modified xylose solution. Therefore, it led to the elasticity of the hydrogels increased from G-0 to G-0.7. Whereas the hydrogels H-30, H-50, H-70, and H-90 had the same water content, more hydrogen bonds and electrostatic interactions were formed with the increasing concentration of modified xylose. It formed tighter and tougher network structure during the preparation of the composite hydrogels,

which resulted in the decreasing elasticity and the increasing compression stress of the hydrogels from H-30 to H-90.
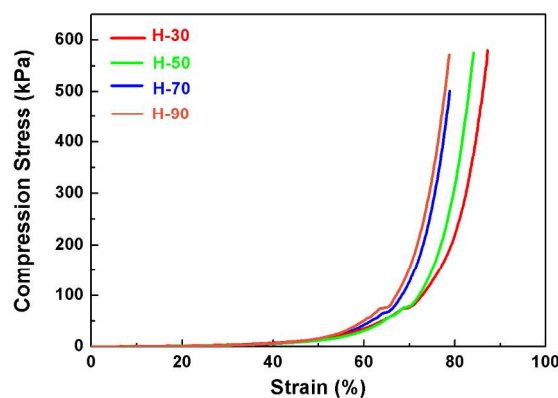
Fig. 9 Compression stress-strain curves of hydrogels H-30, H-50, H-70, and H-90.

Thermal stability

Thermal gravimetric analysis (TGA) was carried out to investigate the thermal properties of the materials and composite hydrogels. TGA curves of xylose (a), methylguanidine hydrochloride (b), modified xylose (c), MMT (d) and hydrogel (e) were illustrated in Fig. 10. As is shown in the TGA curve of xylose, it started to degradation when the temperature reached about 220 °C, and the weight loss of xylose mainly occurred at 220-500 °C. Methylguanidine hydrochloride possessed thermal stability below 300 °C (Fig. 10b). But its weight declined sharply by 96% from 280 to 370 °C. When the temperature continued to be heated to 500 °C, the methylguanidine hydrochloride sample was decomposed completely. The curve of modified xylose was introduced in Fig. 10c, compared with the curves of xylose (a) and methylguanidine hydrochloride (b), more residual weight was observed in the curve of modified xylose (c). It suggested that the methylguanidine hydrochloride was grafted to xylose successfully, forming new bonds between xylose and methylguanidine hydrochloride with relatively high molecular weight. Therefore, the thermal properties of modified xylose were better than xylose and methylguanidine hydrochloride. As can be seen from the curve of MMT, the initial low temperature weight loss (<100 °C) corresponded to the free water evaporation. In addition, 90% residue weight of MMT still remained when the temperature reached 600 °C, indicating that MMT had excellent thermal stability, which was benefit to flame retardant property of composite hydrogels.[26] From the curve of hydrogel, the weight of hydrogel dropped slowly in the range of 20-600 °C, whereas the weight only decreased 33% during the whole process of thermal decomposition. It indicated that the reagents material dispersed homogeneously and the thermal stability of hydrogel was far more than that of modified xylose due to the addition of inorganic phase MMT.
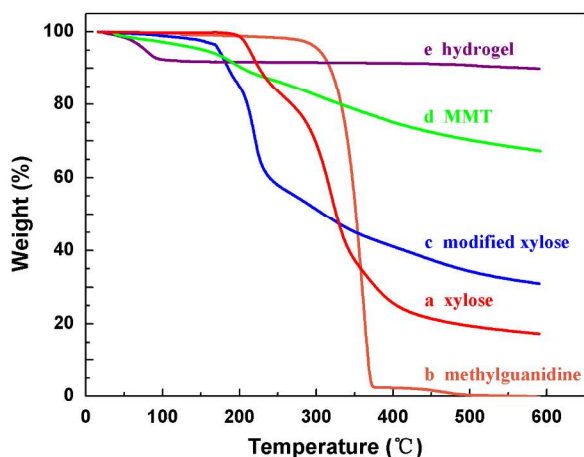
Fig. 10 TGA curves of xylose (a), methylguanidine hydrochloride (b), modified xylose (c), MMT (d), and hydrogel (e).

Conclusions

A convenient, quick, and inexpensive method has been applied to fabricate hydrogels, using xylose as the main subject crosslinking with MMT and PAAS. The prepared xylose-based hydrogels are reproducible and biodegradable. The hydrogels with internal tight porous network structure were prepared by hydrogen bonds and intermolecular interactions instead of traditional covalent bond, which result in that the hydrogels have rapid self-healing ability and show good swelling performance. From the results of compression stress-strain, it was found that elasticity of xylose-based hydrogels increased with the increasing volume of modified xylose solution, and the compression stress increased with the increasing concentration of modified xylose. Furthermore, the xylose-based hydrogels exhibited admirable thermal stability on account of the added MMT nanoplatelets as inorganic phase. These research results revealed that the xylose-based hydrogels make promising applications in many fields. The self-healing property of the hydrogels can prolong the lifespan of materials and reduce the replacement costs due to damage. It can also be used as flame retardant wrapping materials because of its excellent thermal heat resistance. Besides, the composite hydrogel can be used as soil and water humectant on account of its good swelling performance. Thus, the composite hydrogels have a wide range of applications in environmentally friendly materials.

Acknowledgements

Notes and references

[a] Beijing Key Laboratory of Lignocellulosic Chemistry, Beijing Forestry University, Beijing 100083, China. E-mail: fengpeng@bjfu.edu.cn.

[b] State Key Laboratory of Pulp and Paper Engineering, South China University of Technology, Guangzhou, China.

1   Q. Wang, J. L. Mynar, M. Yoshida, E. Lee, M. Lee, K. Okuro, K. Kinbara and T. Aida, *Nature*, 2010, **463**, 339-343.
2   A. J. Ragauskas, C. K. Williams, B. H. Davison, G. Britovsek, J. Cairney, C. A. Eckert, W. J. Frederick, Jr., J. P. Hallett, D. J. Leak, C. L. Liotta, J. R. Mielenz, R. Murphy, R. Templer and T. Tschaplinski, *Science*, 2006, **311**, 484-489.
3   N. U. Nair and H. Zhao, *ChemBioChem*, 2008, **9**, 1213-1215.
4   K. Tuohy, G. Rouzaud, W. Bruck and G. Gibson, *Curr. Pharm. Design*, 2005, **11**, 75-90.
5   J. Parajó, G. Garrote, J. Cruz and H. Dominguez, *Trends Food Sci. Tech.*, 2004, **15**, 115-120.
6   T. Werpy, G. Petersen, A. Aden, J. Bozell, J. Holladay, J. White, A. Manheim, D. Eliot, L. Lasure and S. Jones in *Top value added chemicals from biomass. Volume 1-Results of screening for potential candidates from sugars and synthesis gas*, *Vol.* DTIC Document, 2004.
7   P. Gupta, K. Vermani and S. Garg, *Drug Discov. Today*, 2002, **7**, 569-579.
8   M. P. Lutolf, *Nat. Mater.*, 2009, **8**, 451-453.
9   S. Van Vlierberghe, P. Dubruel and E. Schacht, *Biomacromolecules*, 2011, **12**, 1387-1408.
10 B. V. Slaughter, S. S. Khurshid, O. Z. Fisher, A. Khademhosseini and N. A. Peppas, *Adv. Mater.*, 2009, **21**, 3307-3329.
11 J. N. Hunt, K. E. Feldman, N. A. Lynd, J. Deek, L. M. Campos, J. M. Spruell, B. M. Hernandez, E. J. Kramer and C. J. Hawker, *Adv. Mater.*, 2011, **23**, 2327-2331.
12 S. Tamesue, M. Ohtani, K. Yamada, Y. Ishida, J. M. Spruell, N. A. Lynd, C. J. Hawker and T. Aida, *J. Am. Chem. Soc.*, 2013, **135**, 15650-15655.
13 N. Peppas, Y. Huang, M. Torres-Lugo, J. Ward and J. Zhang, *Annu. Rev. Biomd. Eng.*, 2000, **2**, 9-29.
14 K. Haraguchi and T. Takehisa, *Adv. Mater.*, 2002, **14**, 1120.
15 A. Bortolin, F. A. Aouada, L. H. Mattoso and C. Ribeiro, *J. Agr. Food Chem.*, 2013, **61**, 7431-7439.
16 H. Van Hoang and R. Holze, *Chem. Mater.*, 2006, **18**, 1976-1980.
17 S. Khatana, A. K. Dhibar, S. Sinha Ray and B. B. Khatua, *Macromol. Chem. Phys.*, 2009, **210**, 1104-1113.
18 T. Wu, T. Xie and G. Yang, *J. Appl. Polym. Sci.*, 2010, **115**, 2773-2778.
19 S. S. Ray and M. Okamoto, *Prog. Polym. Sci.*, 2003, **28**, 1539-1641.
20 D. W. Thompson and J. T. Butterworth, *J. Colloid Interf. Sci.*, 1992, **151**, 236-243.
21 K. Okuro, K. Kinbara, K. Tsumoto, N. Ishii and T. Aida, *J. Am. Chem. Soc.*, 2009, **131**, 1626-1627.
22 N. Uchida, K. Okuro, Y. Niitani, X. Ling, T. Ariga, M. Tomishige and T. Aida, *J. Am. Chem. Soc.*, 2013, **135**, 4684-4687.
23 M. A. Kostiainen, O. Kasyutich, J. J. Cornelissen and R. J. Nolte, *Nat. Chem.*, 2010, **2**, 394-399.
24 Y. Guan, B. Zhang, J. Bian, F. Peng and R.-C. Sun, *Cellulose*, 2014, **21**, 1709-1721.
25 M. Pandey, N. Mohamad and M. C. I. M. Amin, *Mol. Pharmaceut.*, 2014, **11**, 3596-3608.

RSC Advances Accepted Manuscript

26 Y. Guan, B. Zhang, X. Tan, X.-M. Qi, J. Bian, F. Peng and R.-C. Sun, *ACS Sustain. Chem. Eng.*, 2014, **2**, 1811-1818.

27 K. Parida, G. B. B. Varadwaj, S. Sahu and P. C. Sahoo, *Ind. Eng. Chem. Res.*, 2011, **50**, 7849-7856.

28 N. Bhattarai, J. Gunn and M. Zhang, *Adv. Drug Deliver. Rev.*, 2010, **62**, 83-99.

29 K. Crompton, J. Forsythe, M. Horne, D. Finkelstein and R. Knott, *Soft Matter*, 2009, **5**, 4704-4711.

34 3362.

30 A. Phadke, C. Zhang, B. Arman, C.-C. Hsu, R. A. Mashelkar, A. K. Lele, M. J. Tauber, G. Arya and S. Varghese, *P. Natl. Acad. Sci.*, 2012, **109**, 4383-4388.

31 Y. Huang, M. Zeng, J. Ren, J. Wang, L. Fan and Q. Xu, *Colloid. Surface. A*, 2012, **401**, 97-106.

32 J. Shen, B. Yan, T. Li, Y. Long, N. Li and M. Ye, *Soft Matter*, 2012, **8**, 1831-1836.

33 H. P. Cong, P. Wang and S.-H. Yu, *Chem. Mater.*, 2013, **25**, 3357-